Order formation and superfluidity of excitons in type-II semiconductor quantum wells

T. Iida and M. Tsubota
Department of Physics, Osaka City University, Sumiyoshi-ku, Osaka 558-8585, Japan
(Received 4 January 1999)

The condensed state and superfluidity of excitons in type-II semiconductor quantum wells (QW's) are investigated theoretically. Since the excitons in type-II QW's have translational motion along the layer, the assembly of them is regarded as an interacting dilute quasi-two-dimensional Bose gas. This system is advantageous for our purpose because those excitons have a long lifetime of the order of 10^{-6} s, and their transport mechanism can be directly studied in experiments by observing electric current since the excitons consist of spatially separated electron-hole pairs. Using the exciton wave functions obtained by the variational method, the exciton-exciton interaction is calculated and found to be repulsive when the thickness of the QW is thinner than a critical value. To illustrate the situation, we carry out the numerical computation adopting a model system with material constants appropriate to GaAs/AlAs type-II QW's. The basic equation for the phase of the condensate wave function is derived when the exciton system is irradiated by a weak laser light at zero temperature. Solving the equation in the presence of the external current J_{ex}, we study the stationary spatial pattern of the phase of the condensate wave function. It is shown that there appears a vortex lattice with a net supercurrent when J_{ex} is larger than a critical value; the period of the lattice is determined as a function of J_{ex}. We calculate the magnetic field induced by the current in the vortex lattice, and discuss a possibility of an experimental observation of the critical current. Such a direct observation of the exciton transport will provide unambiguous experimental evidence for the superfluidity of excitons. [S0163-1829(99)15931-9]

I. INTRODUCTION

There has been a growing interest in many-body effects in the optically excited electron-hole system in semiconductors because the system is expected to exhibit macroscopic quantum coherent phenomena.[1,2] In the high-density regime, the electron-hole system is regarded as a two-component Fermi liquid in which the cooperative pairing of electrons and holes arises in momentum space at low temperatures, quite similar to the BCS state in superconductors,[1–5] while, in the low-density regime, the electron-hole pairs are regarded as well-defined excitons which are the bound states in the real space. In a dense gas of excitons where the excitons are still regarded as bosons, their Bose-Einsten condensation (BEC) is expected.[1]

Superfluidity in liquid ^{4}He is intimately connected with BEC. However, in liquid ^{4}He, the quantum-statistical features associated with BEC are masked by the effects due to the strong particle-particle interactions. More dilute systems have been required to study the connection between Bose-Einstein statistics and superfluidity. The recent successful observations of BEC in dilute alkali atoms have opened the door to study weakly interacting Bose gas experimentally.[6] In addition to the assemblies of alkali atoms, many candidates for BEC can be listed, as shown in Ref. 7. A significant place in this list is occupied by excitons. The reasons in favor of searching the superfluid transition in exciton systems are as follows: (1) A light effective mass allows condensation at a low critical density, so that the system can be regarded as a dilute Bose gas even in the condensed state. For example, in the case of excitons in Cu_2O with a Bohr radius $a_x \simeq 7$ Å, the critical density n_c is $\sim 10^{17}\,\mathrm{cm}^{-3}$ at $T \sim 3$ K and then $n_c a_x^3 \ll 1$, in contrast with $n_c \sim 10^{22}$ in the liquid ^{4}He with an average interparticle distance ~4.4 A. (2) The system can be monitored by convenient optical measurements. (3) There will be a possibility of realizing crossover from the momentum space pairing to the real-space pairing because the exciton density can be controlled over a wide range.

In the recent study by Snoke and Wolfe[8] of the time-resolved luminescence of excitons in Cu_2O, they observed a gradual evolution of exciton distribution from a classical to a Bose quantum degenerate regime, which likely represents the experimental signature of the BEC of excitons. In a subsequent experiment, Fortin and co-workers[9,10] investigated the exciton system in Cu_2O by measuring the time- and space-resolved spectroscopies. They found supersonic ballistic exciton propagation over a macroscopic distance. This ballistic propagation has been interpreted from two different standpoints. One interpretation is based on the BEC and the transition of exciton gas to a superfluid state.[11–13] Another interpretation is based on the phonon wind model, in which excitons are dragged in the crystal by a flow of nonequilibrium ballistic phonons.[14,15] So far, conclusive experimental evidence verifying the transport mechanism of excitons has not yet been obtained. The charge neutrality of excitons prevents us from studying the exciton transport directly by the observation of electric current.

In the present work, in order to overcome such a difficulty, we propose an exciton system in a type-II quantum well (QW), and investigate the quantum coherent phenomena of excitons (the very preliminary result was reported in Ref. 16). Our system is similar to the electron-hole system in coupled layered semimetals with electron and hole conductions separated by a thin insulating layer, which was studied in Ref. 17.

In the type-II QW, the exciton consists of an electron and a hole which are confined separately in two adjacent layers

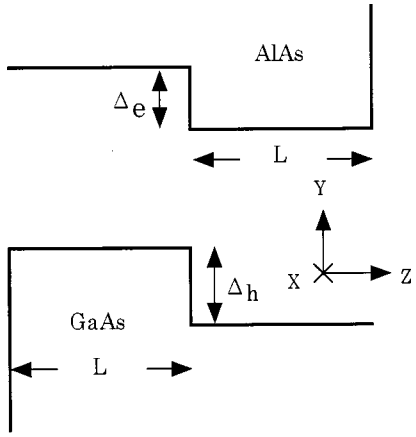

FIG. 1. The type-II quantum-well structure. As a model system, a set of parameter values of GaAs/AlAs are assumed (see text).

by confinement potentials. The center of mass of the exciton moves along the layer. Therefore the translational motion is regarded as being quasi-two-dimensional (2D), and is accompanied by currents flowing in the opposite directions in the electron and the hole layers. This fact makes it possible for us to observe the exciton transport by measuring the electric current. The system offers the additional advantage of realizing the condensed states of excitons. The spatially separated distributions of electrons and holes greatly reduce the probability of electron-hole recombination decay; typically the lifetime of excitons is $\sim 10^{-6}$ s. In Sec. II, we calculate the exciton states in type-II QW (see Fig. 1) by a variational method based on the effective-mass approximation, adopting a model system with parameter values of a GaAs/AlAs QW with each layer of thickness L. On the basis of the results, we study the exciton-exciton interaction, which plays an essential role in obtaining the stable condensate of excitons. The result shows that the exciton-exciton interaction is repulsive when L is smaller than a certain critical value. The assembly of excitons in our system can be considered to be approximately an interacting dilute 2D Bose gas as long as the exciton density is small compared to a_x^{-2}, a_x being the exciton radius. The exciton condensed state is characterized by a finite ensemble average of the field operator $\psi(\mathbf{R})$, where $\mathbf{R}$ is the position vector in 2D space; $\psi(\mathbf{R}) \equiv \langle \psi(\mathbf{R}) \rangle$ is called the condensate wave function. In Sec. III, we derive the basic equations for the condensate wave function of excitons in a type-II QW which is irradiated by a weak laser light at absolute zero temperature; the case of finite temperature will be studied in a future work. In Sec. IV, we consider a system where the electron and hole layers are connected in series. The basic equations obtained in Sec. III are supplemented by the boundary conditions determined at the boundaries of the system for a given external current J_{ex}. Solving the equations, we study the current distribution pattern caused by the spatial variation of the phase of $\psi(\mathbf{R})$, and show that there appears a vortex lattice with net supercurrent when J_{ex} is larger than a critical value. We also calculate the magnetic field induced by the current in the vortex-lattice state. Furthermore, order estimations are carried out for the critical current and the magnetic filed, which shows that it will be possible to observe them experimentally. The experimental observation of the critical current will give unambiguous evidence on the superfluidity of excitons.

II. EXCITONS IN A TYPE-II QUANTUM WELL

We consider a simple model of a type-II quantum well in which electrons and holes are confined separately within two adjacent layers with the same thickness L. The claddings of both layers are assumed to be formed by high-barrier materials. The model band scheme is shown in Fig. 1. A GaAs/AlAs quantum-well structure with thickness less than $\sim$36 A is a typical experimentally accessible example in which the spatially separated electron-hole system is realized; in this case, the lowest electron state originating from X states of AlAs is localized within the AlAs layer, while the lowest hole state built up from Γ states of GaAs is localized within the GaAs layer.[18]

The exciton wave functions are written as

$$\Psi_{\mathbf{K}}(\mathbf{r}_e,\mathbf{r}_h) = e^{i\mathbf{K}(\alpha_e\boldsymbol{\rho}_e+\alpha_h\boldsymbol{\rho}_h)}\varphi(\boldsymbol{\rho},z_e,z_h),$$

$$\varphi(\boldsymbol{\rho},z_e,z_h) = \exp(ik_c z_e) f(\boldsymbol{\rho},z_e,z_h), \tag{1}$$

where the z axis is taken along the growth direction (Fig. 1); the subscripts e and h indicate, respectively, the electron and the hole; the wave vector $\mathbf{K}$, the position vector $\boldsymbol{\rho}_a$ ($a=e,h$), and $\boldsymbol{\rho}=\boldsymbol{\rho}_e-\boldsymbol{\rho}_h$ are those in the xy plane; and $\exp(ik_c z_e)$ is the phase factor coming from the conduction-band bottom. $\alpha_a = m_{axy}/M$ and $M = m_{exy}+m_{hxy}$, m_{axy} being the effective mass in the xy plane.

The wave function $f(\boldsymbol{\rho},z_e,z_h)$ satisfies the effective-mass equation

$$\left[H_e+H_h-\frac{\hbar^2}{2m_r}\nabla_\rho^2 - V(\boldsymbol{\rho},z_e-z_h)\right] f(\boldsymbol{\rho},z_e,z_h)$$

$$= \epsilon f(\boldsymbol{\rho},z_e,z_h). \tag{2}$$

Here $1/m_r = 1/m_{exy}+1/m_{hxy}$ and

$$H_a = -\frac{\hbar^2}{2m_{az}}\frac{\partial^2}{\partial z_a^2} + W^a(z_a) \quad (a=e,h),$$

$$V(\boldsymbol{\rho},z_e-z_h) = \frac{e^2}{\varepsilon\sqrt{\boldsymbol{\rho}^2+(z_e-z_h)^2}}, \tag{3}$$

where m_{az} is the effective mass along the z direction, and $W^a(z_a)$'s are the confinement potentials. Since we need only the lowest electron and hole states in the following discussion, we ignore the cladding effects and approximate the confinement potensitials as

$$W^e(z_e) = \begin{cases} -\Delta_e, & 0 \le z_e \le L \\ 0 & \text{otherwise,} \end{cases}$$

$$W^h(z_h) = \begin{cases} -\Delta_h, & -L \le z_h \le 0 \\ 0 & \text{otherwise,} \end{cases} \tag{4}$$

where $\Delta_{e(h)}$ are the band discontinuities. In the Coulomb interaction between electron and hole in Eq. (3), we neglect image-charge effects.

We consider the situation where the confinement effects for the electrons and holes are large enough compared with

the electron-hole Coulomb interaction, and then the lowest exciton state is composed of the lowest states of the confined electron and hole. As a first step, we calculate the lowest electron and hole states, adopting the trial functions

$$u_a(z_a,\eta_a)=\left(\frac{2}{\pi\eta_a^2}\right)^{1/4} e^{-(z_a-L_a/2)^2/\eta_a^2} \quad (L_e=L, L_h=-L), \tag{5}$$

where the η_a's are variational parameters used to minimize the energies

$$e_a(\eta_a)\equiv\langle u_a|H_a|u_a\rangle=\frac{\hbar^2}{2m_a\eta_a^2}-\Delta_a\,\mathrm{erf}\left(\frac{L}{\sqrt{2}\eta_a}\right), \tag{6}$$

where erf(x) is the error function:

$$\mathrm{erf}(x)=\frac{2}{\sqrt{\pi}}\int_0^x \exp(-t^2)dt. \tag{7}$$

In the next step, using the obtained states $u_a(z_a,\eta_a)$, we assume the trial function for the exciton state as

$$f(\boldsymbol{\rho},z_e,z_h)=\varphi(\boldsymbol{\rho})u_e(z_e,\eta_e)u_h(z_h,\eta_h),$$

$$\varphi(\rho)=\frac{2}{\sqrt{2\pi}a_x}e^{-\rho/a_x}, \tag{8}$$

where the the two-dimensional exciton radius a_x is introduced as the variational parameter. By using the Fourier transforms of $\varphi(\boldsymbol{\rho})$ and $V(\boldsymbol{\rho},z_e-z_h)$,

$$\varphi(q)=\frac{\sqrt{8\pi a_x^2}}{[1+(a_xq)^2]^{3/2}}, \quad V(q,z_e-z_h)=V_q e^{-q|z_e-z_h|},$$

$$V_q=\frac{2\pi e^2}{\varepsilon q}, \tag{9}$$

the exciton energy ϵ is calculated to be $\epsilon(\eta_e,\eta_h,a_x)=e_e(\eta_e)+e_h(\eta_h)-E_x$, where E_x is the exciton binding energy defined by

$$E_x=-\left[\frac{\hbar^2}{2m_ra_x^2}+W^{eh}(\eta_e,\eta_h,a_x)\right]. \tag{10}$$

Here

$$W^{eh}(\eta_e,\eta_h,a_x)=-\frac{1}{2\pi}\int_0^\infty dq\, qV_q\frac{f_{eh}(q)}{[1+(a_xq/2)^2]^{3/2}} \tag{11}$$

with

$$f_{ab}(q)=\int_{-\infty}^{\infty}dz_a\int_{-\infty}^{\infty}dz_b' e^{-q|z_a-z_b'|}|u_a(z_a,\eta_a)|^2|u_b(z_b',\eta_b)|^2. \tag{12}$$

Minimizing the exciton energy ϵ with respect to the exciton radius a_x, we finally obtain the energy for the exciton state $\psi_{\mathbf{K}}(\mathbf{r}_e,\mathbf{r}_h)$ as follows:

$$E(\mathbf{K})=E_g+\frac{\hbar^2K^2}{2M}-E_x,$$

$$E_g=\varepsilon_g+[\Delta_e+e_e(\eta_e)]+[\Delta_h+e_h(\eta_h)], \tag{13}$$

where ε_g is the indirect band gap and E_g is the electron-hole excitation energy when the exciton effect is neglected.

By adopting the exciton states $\Psi_{\mathbf{K}}(\mathbf{r}_e,\mathbf{r}_h)$'s obtained above as a complete set of one-exciton states, the Hamiltonian of the many-exciton system may be derived. The Hamiltonian describes the translational motion of excitons in the xy plane, and involves the exciton-exciton interaction whose matrix element is given in the form[19,20]

$$W(\mathbf{K},\mathbf{K}',\mathbf{P})=W_d(\mathbf{P})+W_x(\mathbf{K},\mathbf{K}',\mathbf{P}), \tag{14}$$

where $\mathbf{K},\mathbf{K}',\mathbf{P}$ are the wave vectors in the xy plane, $W_d(\mathbf{P})$ is the direct interexcitonic interaction, and $W_x(\mathbf{K},\mathbf{K}',\mathbf{P})$ comes from the exchange of the fermions belonging to different excitons. In the case of the low concentration at $T=0$, the interaction between the low-energy excitons makes the dominant contribution. Then we assume that the exciton-exciton interaction is approximated by $W_x(K,K',P)\approx W_x(0,0,0)$; by using the explicit expression given in Refs. 19 and 20, the matrix elements are calculated to be

$$W_d(0)=0, \tag{15}$$

$$W_x(0,0,0)=-\sum_{\mathbf{q},\mathbf{q}_1}[V_q^{ee}+V_q^{hh}]\varphi(\mathbf{q}_1)^2\varphi(\mathbf{q}_1-\mathbf{q})^2 +2\sum_{\mathbf{q},\mathbf{q}_1}V_q^{eh}\varphi(\mathbf{q}_1)^3\varphi(\mathbf{q}_1-\mathbf{q}), \tag{16}$$

where $V_{ab}=f_{ab}(q)V_q$, $f_{ab}(q)$ and V_q being given in Eqs. (12) and (9), respectively; the Coulomb interaction is modified by the overlap integral of the quantum-well electron and hole wave functions in the z direction.

If the overlap integrals $f_{ab}(q)$'s were unity in Eq. (16), W_x would be of the same form as in a two-dimensional case where the electrons and holes are distributed in the same two-dimensional space. In this case, W_x is calculated as[21]

$$W_x(0,0,0)=E_x^{2D}(a_x^{2D})^2\left\{8\pi\left(1-\frac{315\pi^2}{4096}\right)\right\}, \tag{17}$$

with $E_x^{2D}=e^2/\varepsilon a_x^{2D}$ and $a_x^{2D}=\hbar^2\varepsilon/2m_re^2$, and then W_x yields the repulsive exciton-exciton interaction. While in our system, the effects of the spatially separated electron and hole distributions play an essential role; as the thickness increases, the overlap integral f_{eh} decreases although f_{ee} and f_{hh} are almost unaltered. Then there is a possibility that W_x gives the attractive interaction when the thickness becomes large. In order to observe such a characteristic behavior, we carry out a numerical computation of the exciton states using the exciton wave functions given above; our purpose is not a detailed numerical study of quantum-well excitons, but an illustration of the quantitative features of our system.

As a model system, we adopt a set of parameter values of GaAs/AlAs: $m_{ez}=1.1m$, $m_{exy}=0.19m$, and $m_{hz}=m_{hxy}=0.37m$, m being the free-electron mass: $\varepsilon=12.53$.[18] The values of the band discontinuities are $\Delta_e=0.260$ eV, and

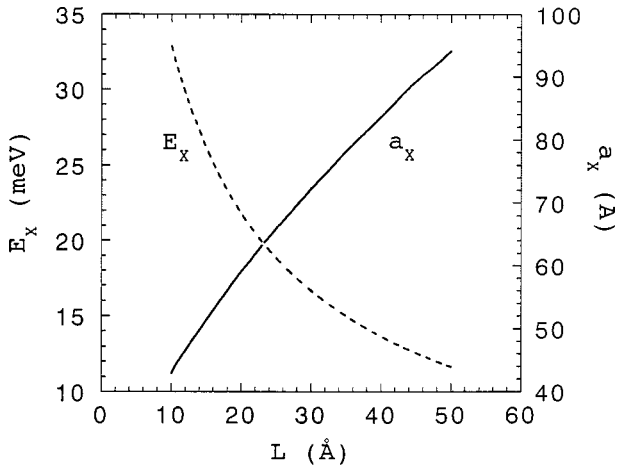

FIG. 2. Thickness, L, dependence of the exciton binding energy E_x (dashed curve) and the in-plane exciton radius a_x (solid curve).

$\Delta_h = 0.548$ eV, which are estimated from the relevant band parameter values[22] using the well-known band-offset ratios $Q_v = 0.34$ and $Q_c = 0.66$ for the valence and conduction bands, respectively.

The computed thickness dependence of the exciton binding energy and the in-plane exciton radius are shown in Fig. 2. The results are easily understood from the effects of the spatial separation of the electron and hole distributions. The computed exciton-exciton interaction $W_x(0,0,0)$ is plotted in Fig. 3 as a function of L. The essential point is that there exists a critical thickness $L_c \simeq 28$ A, and the exciton-exciton interaction is repulsive when L is smaller than L_c. This is a necessary condition for the exciton-condensed state to be stable.

III. BASIC EQUATION OF A CONDENSED EXCITON SYSTEM

Let us consider the many-exciton system in a type-II quantum well which is irradiated by a weak laser light. We shall confine ourselves to the case at absolute zero temperature, where the concentration is assumed to be sufficiently

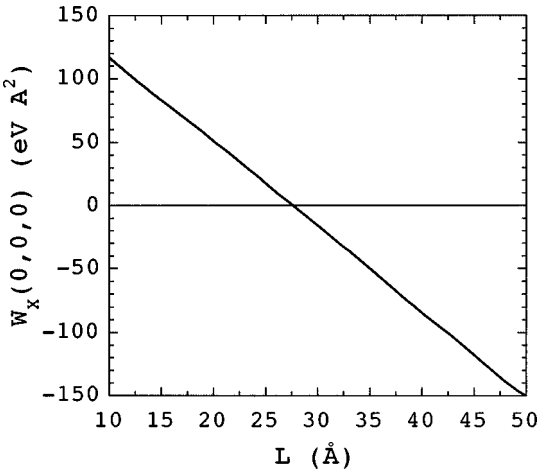

FIG. 3. The exciton-exciton interaction $W_x(0,0,0)$ as a function of thickness L, which is computed with using the exciton wave functions obtained by the variational method.

low so that an exciton can be regarded as a boson. The excitons are assumed to be in the lowest state of the relative motion, and the exciton-exciton interaction is approximated by $W(\mathbf{K},\mathbf{K}',\mathbf{P}) \approx W_x(0,0,0)(\equiv W)$ as discussed in Sec. II. The Hamiltonian for the translational motion of excitons is given as

$$H = \int d\mathbf{R}\, \psi^\dagger(\mathbf{R}) \left[-\frac{\hbar^2}{2M}\nabla_R^2 + (E_{gx} - \mu) \right] \psi^\dagger(\mathbf{R}) + \frac{1}{2}\int d\mathbf{R}_1 d\mathbf{R}_2 \psi^\dagger(\mathbf{R}_1)\psi(\mathbf{R}_2) V(\mathbf{R}_1 - \mathbf{R}_2)\psi^\dagger(\mathbf{R}_2)\psi(\mathbf{R}_1) + H_L, \tag{18}$$

where $E_{gx} = E_g - E_x$, $\psi^\dagger(\mathbf{R})$ and $\psi(\mathbf{R})$ are the field operators for the excitons, $\mathbf{R}$ being the position vector in the xy plane, and $V(\mathbf{R}_1 - \mathbf{R}_2) = W\delta(\mathbf{R}_1 - \mathbf{R}_2)$. The Hamiltonian H_L is the interaction with the weak laser light which is treated as a classical monochromatic field with frequency ω_L in the rotating-wave approximation:

$$H_L = -\int d\mathbf{R}[g_L^* e^{-i\omega_L t}\psi^\dagger(\mathbf{R}) + g_L e^{i\omega_L t}\psi(\mathbf{R})]. \tag{19}$$

By the unitary transformation $H = U^{-1}(t) H U(t)$ with

$$U(t) = \exp\left[-i\omega_L t \int d\mathbf{R}\, \psi^\dagger(\mathbf{R})\psi(\mathbf{R}) \right], \tag{20}$$

we can eliminate the time dependence of H_L, and have

$$H = \int d\mathbf{R}\, \psi^\dagger(\mathbf{R}) \left[-\frac{\hbar^2}{2M}\nabla_R^2 - \mu^* \right] \psi(\mathbf{R}) + \frac{1}{2}\int d\mathbf{R}_1 d\mathbf{R}_2 \psi^\dagger(\mathbf{R}_1)\psi(\mathbf{R}_2) V(\mathbf{R}_1 - \mathbf{R}_2)\psi^\dagger(\mathbf{R}_2)\psi(\mathbf{R}_1) - \int d\mathbf{R}[g_L^*\psi^\dagger(\mathbf{R}) + g_L\psi(\mathbf{R})], \tag{21}$$

where $\mu^* \equiv \mu - (E_{gx} - \hbar\omega_L)$, which may be regarded as the effective chemical potential.

To describe the condensed state, let us introduce the average $\Psi(\mathbf{R}) \equiv \langle \psi(\mathbf{R}) \rangle$ and the deviation operator $\varphi(\mathbf{R}) \equiv \psi(\mathbf{R}) - \Psi(\mathbf{R})$. Since we consider a stationary assembly of excitons at $T = 0$, it is reasonable to assume that almost all the excitons are condensed and the operator φ may be considered a small correction to Ψ. Substituting $\psi(\mathbf{R}) = \Psi(\mathbf{R}) + \varphi(\mathbf{R})$ into Eq. (21) and expanding H in powers of φ and $\varphi^\dagger$, we obtain

$$H = H_0 + H_1 + H_2, \tag{22}$$

where

$$H_0 = \int d\mathbf{R}\, \Psi^*(\mathbf{R}) \left\{ -\frac{\hbar^2}{2M}\nabla_R^2 - \mu^* + \frac{1}{2}W|\Psi(\mathbf{R})|^2 \right\} \Psi(\mathbf{R}) - g_L^* \int d\mathbf{R}\, \Psi^*(\mathbf{R}) - g_L \int d\mathbf{R}\, \Psi(\mathbf{R}), \tag{23}$$

$$H_1=\int d\mathbf{R}\,\varphi^{\dagger}(\mathbf{R})\Bigg\{\Bigg[-\frac{\hbar^2}{2M}\nabla_R^2-\mu^*+W|\Psi(\mathbf{R})|^2\Bigg]\Psi(\mathbf{R})-g_L^*\Bigg\}+\int d\mathbf{R}\Bigg\{\Bigg[-\frac{\hbar^2}{2M}\nabla_R^2-\mu^*+W|\Psi(\mathbf{R})|^2\Bigg]\Psi^*(\mathbf{R})-g_L\Bigg\}\varphi(\mathbf{R}), \tag{24}$$

and H_2 contains the quadratic and other higher-order terms of $\varphi(\mathbf{R})$ and $\varphi(\mathbf{R})^{\dagger}$. We require the function $\Psi(\mathbf{R})$ to satisfy the equation

$$\Bigg[-\frac{\hbar^2}{2M}\nabla_R^2-\mu^*+W|\Psi(\mathbf{R})|^2\Bigg]\Psi(\mathbf{R})-g_L^*=0. \tag{25}$$

Then the linear term H_1 vanishes identically, and the Hamiltonian is reduced to be $H=H_0+H_2$. We call the nonlinear equation (25) the Gross-Pitaevskii (GP) equation, although the original GP-equation does not include g_L^* (or g_L). Equation (25) has a form identical to the equation which is obtained by minimizing the energy H_0 with respect to $\Psi^*(\mathbf{R})$.

The condensate wave function is written as $\Psi(\mathbf{R})=|\Psi(\mathbf{R})|\exp[i\theta(\mathbf{R})]$. From Eq. (25), we have coupled equations for the amplitude and the phase:

$$-\frac{\hbar^2}{2M}\{\nabla_R^2|\Psi|-|\Psi|(\nabla_R\theta)^2\}-\mu^*|\Psi|+W|\Psi|^3-|g_L|\cos(\theta+\chi)=0, \tag{26}$$

$$-\frac{\hbar^2}{2M}\{|\Psi|\nabla_R^2\theta+2\nabla_R|\Psi|\nabla_R\theta\}+|g_L|\sin(\theta+\chi)=0, \tag{27}$$

where we put $g_L=|g_L|\exp(i\chi)$.

The presence of a finite amplitude of $|\Psi|>0$ serves the criterion for the condensed state, and the phase θ is the velocity potential of the superflow of the condensed excitons. In the absence of interaction with the laser light, the uniform condensed state $\Psi(\mathbf{R})=\sqrt{n_0}$ is a solution of the coupled equations, and the effective chemical potential is given by $\mu^*=\mu-E_{gx}=n_0W$. This means that W must be repulsive; otherwise the system is to be unstable. In the presence of interaction with light, it is reasonable to assume that the condensate wave function has a form $\Psi(\mathbf{R})=\sqrt{n_0}\exp[i\theta(\mathbf{R})]$ and the effective chemical potential is approximated by $\mu^*=\mu-(E_{gx}-\hbar\omega_L)\simeq n_0W$ when the condition $g_L/n_0^{2/3}W\ll 1$ is satisfied.

IV. VORTEX-LATTICE FORMATION AND SUPERFLUIDITY

Under the assumption given in Sec. III, the phase of the condensate of excitons obeys the equation

$$-\frac{\hbar^2\sqrt{n_0}}{2M}\nabla_R^2\theta+|g_L|\sin(\theta+\chi)=0. \tag{28}$$

The superflow of the condensed excitons is given by

$$\mathbf{j}(\mathbf{R})=\frac{\hbar}{2iM}[\Psi^*\nabla_R\Psi-(\nabla_R\Psi)^*\Psi]=n_0\mathbf{v}_s(\mathbf{R}),$$

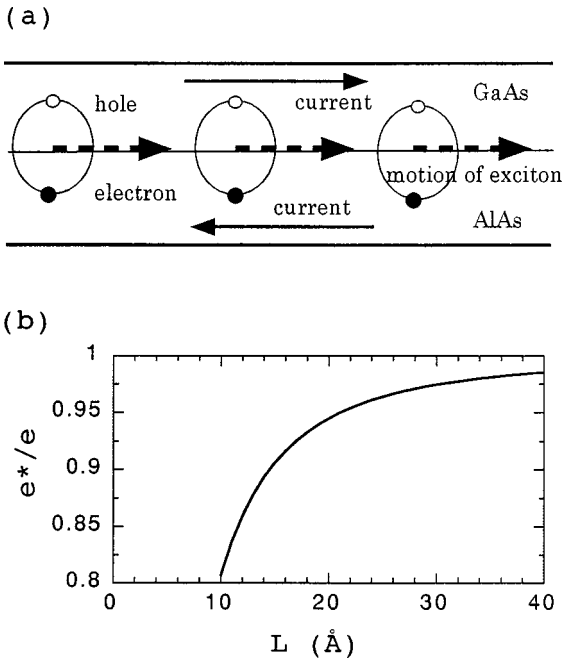

FIG. 4. (a) Schematic illustration of the electric currents which flow in the electron and hole layers accompanying the exciton translational motion. (b) The effective charge e^* in the electron (hole) layer as a function of thickness L, which is computed with using the exciton wave functions obtained by the variational method.

$$\mathbf{v}_s(\mathbf{R})\equiv\frac{\hbar}{M}\nabla_R\theta. \tag{29}$$

The translational motion of excitons is accompanied by electric currents in the hole and the electron layers as depicted in Fig. 4(a). Using the wave function of the exciton, the effective charge in each layer is given as follows:

$$e^*=e\int_0^{\infty}dz[|u_e(z)|^2-|u_h(z)|^2]. \tag{30}$$

The computed effective charge in our model system is shown in Fig. 4(b); we observe that the effective charge is spatially separated significantly for $L>10$ A.

The supercurrents which flow in the electron and hole layers are the same in magnitude but in opposite directions from each other; in the hole layer, the supercurrent is given as

$$\mathbf{J}(\mathbf{R})=e^*n_0\mathbf{v}_s(\mathbf{R}). \tag{31}$$

The creation and destruction of excitons through the interaction H_L causes the effective interlayer current I_T. The interlayer current which flows from the electron layer to the hole layer is calculated by a method similar to that in Ref. 17:

$$I_T=-i(e^*/\hbar)\langle[N_{\mathrm{ex}},H]\rangle=-i(e^*/\hbar)\langle[N_{\mathrm{ex}},H_L]\rangle=\frac{2e^*\sqrt{n_0}}{\hbar}|g_L|\sin(\theta+\chi), \tag{32}$$

where $N_{\mathrm{ex}}(\mathbf{R})=\psi^{\dagger}(\mathbf{R})\psi(\mathbf{R})$. Furthermore, by multiplying Eq. (28) by $2e^*\sqrt{n_0}/\hbar$ and using Eq. (31), it is easily shown that the intralayer current J and the interlayer current I_T satisfy the continuity equation[17]

$$\nabla \mathbf{J} - I_T = 0. \tag{33}$$

Now we set up our system by connecting the hole and electron layers at $x = L_x$ in series, and suppose that an external current $J_{\rm ex}$ flows into the hole layer at $x=0$. The current will be able to flow in the hole and electron layers, and finally flows out of the electron layer at $x=0$. Since the system is uniform in the y direction and the current depends only on x, the basic equations (28) and (31) are reduced to

$$2\lambda^2 \frac{d^2\phi(x)}{dx^2} = \sin 2\phi(x), \quad \lambda^2 \equiv \frac{\hbar^2 \sqrt{n_0}}{2M|g_L|}, \tag{34}$$

$$J(x) = e^* n_0 v_s(x), \quad v_s(x) = \frac{2\hbar}{M} \frac{d\phi(x)}{dx}, \tag{35}$$

where we have defined $2\phi \equiv \theta + \chi$.

The sine-Gordon equation (34) has a conserved quantity E_T equivalent to the total energy

$$E_T = \lambda^2 \left(\frac{d\phi}{dx} \right)^2 + \frac{1}{2} \cos 2\phi. \tag{36}$$

The solutions are classified into two cases according to the value of E_T: (a) $E_T > \frac{1}{2}$ and (b) $-\frac{1}{2} < E_T < \frac{1}{2}$.

In case (a), the solution of Eq. (34) is given by

$$\cos \phi = -\,\mathrm{sn}\left(\frac{x}{k\lambda}, k \right), \quad k^{-2} \equiv E_T + \frac{1}{2}, \tag{37}$$

where the function sn refers to the Jacobian elliptic function, and the parameter k is subject to the condition $0 < k^2 < 1$. The phase ϕ at $x=0$ is chosen so that $\phi = (2n+1/2)\pi$ with an integer n, and increases monotonically with x. The solution yields the supercurrent

$$J(x) = \frac{2e^* \hbar n_0}{Mk\lambda} \mathrm{dn}\left(\frac{x}{k\lambda}, k \right), \tag{38}$$

which is always positive in spite of oscillating with the periodicity $a(k) = 2\lambda k K(k)$, and then there exists the net supercurrent

$$\overline{J} = \frac{1}{a} \int_0^a J(x)dx = \frac{2\pi e^* \hbar n_0}{Ma}, \tag{39}$$

where $K(k)$ is the complete elliptic integral of the first kind. From Eq. (32), the interlayer current is calculated to be

$$I_T(x) = -2 \frac{2e^* \sqrt{n_0}|g_L|}{\hbar} \mathrm{sn}\left(\frac{x}{k\lambda}, k \right) \mathrm{cn}\left(\frac{x}{k\lambda}, k \right). \tag{40}$$

Then the intralayer and interlayer currents $J(x)$ and $I_T(x)$ form the vortex lattice with the lattice constant $a(k)$ as shown schematically in Fig. 5.

In case (b), the solution of Eq. (34) is given by

$$\cos \phi = -k\,\mathrm{sn}\left(\frac{x}{\lambda}, k \right), \quad k = \sqrt{E_T + \tfrac{1}{2}}. \tag{41}$$

The resulting supercurrent

$$J(x) = \frac{2e^* \hbar k n_0}{M\lambda} \mathrm{cn}\left(\frac{x}{\lambda}, k \right) \tag{42}$$

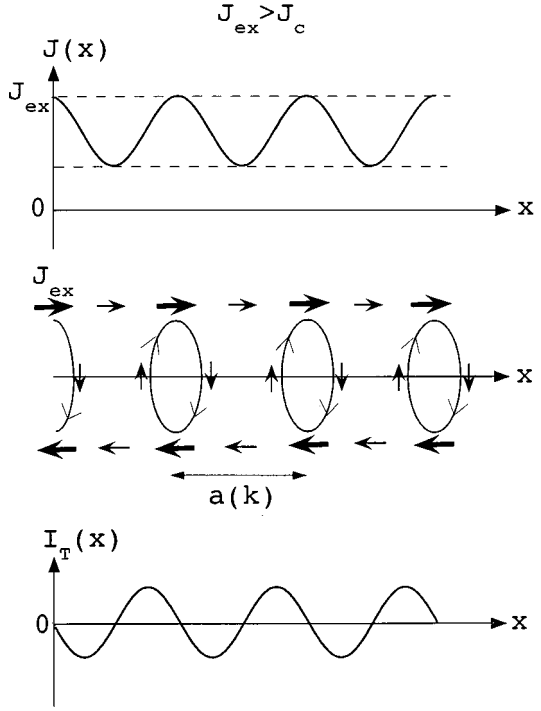

FIG. 5. Schematic illustration of the vortex lattice in the case of $J_{\rm ex} > J_c$. The currents $J(x)$ and $I_T(x)$ are also shown schematically to see how the vortex is constructed by them.

is a periodic function with the lattice constant $b(k) = 4\lambda K(k)$. The interlayer current is given by

$$I_T(x) = -2 \frac{2e^* \sqrt{n_0}|g_L|}{\hbar} k\,\mathrm{sn}\left(\frac{x}{\lambda}, k \right) \mathrm{dn}\left(\frac{x}{\lambda}, k \right). \tag{43}$$

In this case, the intralayer and interlayer currents form the vortex-antivortex lattice, as shown in Fig. 6, and there ap-

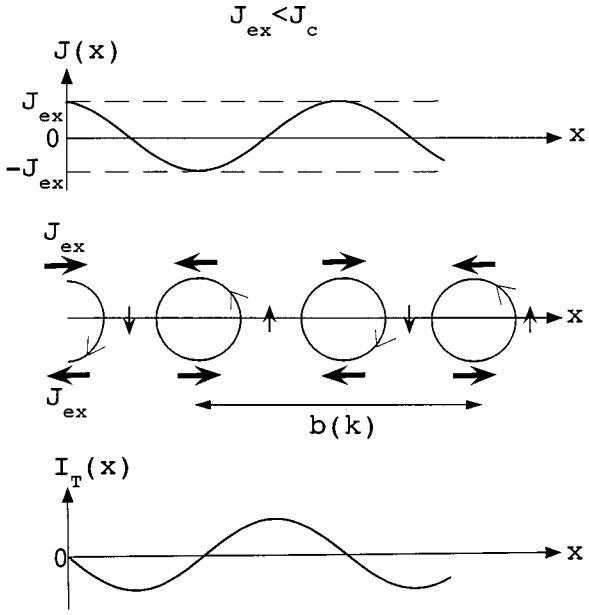

FIG. 6. Schematic illustration of the vortex-antivortex lattice in the case of $J_{\rm ex} < J_c$. The currents $J(x)$ and $I_T(x)$ are also shown schematically to see how the vortex is constructed by them.

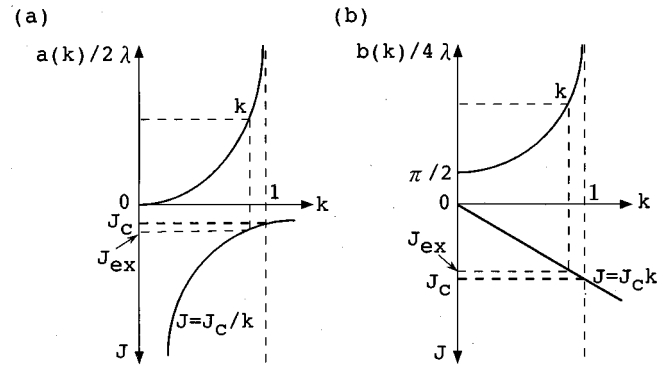

FIG. 7. Schematic diagrams which show how the periods $a(k)$ and $b(k)$ are determined depending on $J_{\rm ex}$ when (a) $J_{\rm ex}>J_c$ and (b) $J_{\rm ex}>J_c$, respectively.

pears no net supercurrent.

The lattice constants $a(k)$ and $b(k)$, which remain undetermined in the above calculation, are determined by the external current. In our system, the current is subject to the boundary condition

$$J(x=0)=J(x=L_x)=J_{\rm ex}. \tag{44}$$

If the vortex lattice with the lattice constant $a(k)=2\lambda kK(k)$ is constructed, the condition

$$L_x=la(k)=2l\lambda kK(k) \tag{45}$$

should be satisfied, where l represents the number of the vortices. The boundary condition (44) is expressed as

$$J_{\rm ex}=\frac{J_c}{k}, \quad J_c\equiv\frac{2e^*\hbar n_0}{M\lambda}=2e^*n_0^{3/4}\left(\frac{2|g_L|}{M}\right)^{1/2}, \tag{46}$$

which determines the lattice constant $a(k)$ as a function of $J_{\rm ex}$; in Fig. 7(a), we present the schematic illustration of the graphical determination of $a(k)$. Since the upper limit of $k=1$ corresponds to $J_{\rm ex}=J_c$, the vortex-lattice solution is possible only when $J_{\rm ex}$ is larger than J_c. From Eq. (45), the number of the vortices is given by $l=(L_x/\lambda)/2kK(k)$. As will be shown later in a numerical analysis, in an actual system with a macroscopic size of L_x, the magnitude of L_x/λ is extremely large, let us say $\sim 10^5$, so that l is practically regarded as the continuous function of $J_{\rm ex}$. If we could construct a mesoscopic system having a sufficiently small size of L_x/λ, say ~ 10, we would be able to observe the vortex entering the system one by one as increasing the external current $j_{\rm ex}$.

A similar analysis is applicable to the vortex-antivortex lattice in case (b), where the system should satisfy the conditions

$$L_x=lb(k), \quad J_{\rm ex}=J_ck. \tag{47}$$

In Fig. 7(b), we show schematically how $b(k)$ is determined. As seen from Fig. 7(b), the solution is possible only when $J_{\rm ex}<J_c$. Thus there exists a critical current J_c defined by Eq. (46) and, at $J_{\rm ex}=J_c$, the system makes a transition from the vortex-antivortex lattice state to a vortex lattice state in which the net supercurrent appears.

Here, it is worthwhile noting the case of infinite system. In this case, the lattice constant is determined by the condition that the free energy should be at a minimum in the presence of the external current. The free-energy for the phase ϕ is written as[16,17]

$$F(\phi)=4|g_L|\sqrt{n_0}\int\left[\lambda^2\left(\frac{d\phi}{dx}\right)^2+\sin^2\phi\right]dx - 2J_{\rm ex}\frac{\hbar}{e^*}\int\frac{d\phi}{dx}dx. \tag{48}$$

The variation $\delta F/\delta\phi=0$ yields the sine-Gordon equation (34). When $E_T>\frac{1}{2}$, the free energy per unit length for the vortex-lattice solution (37) is given by

$$F=\frac{4|g_L|\sqrt{n_0}}{k^2}\left(\frac{2E(k)}{K(k)}+k^2-1\right)-\frac{\pi\hbar J_{\rm ex}}{e^*\lambda kK(k)}, \tag{49}$$

where $E(k)$ is the complete elliptic integral of the second kind. The condition $dF/dk=0$ leads to

$$\frac{E(k)}{k}=\frac{\pi\hbar J_{\rm ex}}{8|g_L|\sqrt{n_0}e^*\lambda}, \tag{50}$$

via which the lattice constant $a(k)=2\lambda kK(k)$ is given as a function of $J_{\rm ex}$. Since $E(k)/k$ is larger than unity, only when $J_{\rm ex}$ exceeds the critical current

$$J_{c,\rm inf}=\frac{8|g_L|\sqrt{n_0}e^*\lambda}{\pi\hbar}=\frac{4e^*n_0^{3/4}}{\pi}\left(\frac{2|g_L|}{M}\right)^{1/2}, \tag{51}$$

the free energy of Eq. (49) become negative for k given by Eq. (50), so that the vortex lattice is formed and the net supercurrent of Eq. (39) appears. It should be noted that the critical current $J_{c,\rm inf}$ is smaller than J_c for the finite system by the factor $2/\pi$. This deference will be interpreted as follows. When $J_{\rm ex}$ exceeds $J_{c,\rm inf}$, the vortex-lattice solution becomes thermodynamically stable. However, a real system with a finite size allows the vortex to enter only when $J_{\rm ex}$ becomes still larger than J_c and the conditions of Eqs. (45) and (46) are satisfied. A similar thing also occurs in the critical magnetic field for the Josephson vortex that appears in the Josephson junction under an applied magnetic field;[23] although the vortex in our system is free from the normal core, it is similar to the Josephson vortex.

The current in the vortex-lattice state is accompanied by the magnetic flux, which plays an essential role in experiments to obtain evidence of the existence of the vortex lattice. The magnetic field is derived from the Maxwell equation $\mathrm{rot}\,\mathbf{B}=(4\pi/c)\mathbf{J}$ and the continuity equation (33),

$$B_y(x)=\frac{4\pi}{c}J(x)=\frac{\Phi_0}{\pi dk\lambda}\,\mathrm{dn}\left(\frac{x}{k\lambda},k\right) \tag{52}$$

for $J_{\rm ex}>J_c$, where $\Phi_0=2\pi\hbar c/e^*$ is the flux quantum and $d=Mc^2/4\pi e^{*2}n_0$. The present flux quantum is twice the usual one coming from Cooper pair in superconductors. The quantity $k\lambda$ represents the effective scale of the length along the layer, while d, which has the dimensions of a length, is presumed to be that of the length along the growth direction. The mean magnetic field accompanying each lattice is given by

$$\overline{B}=\frac{1}{a(k)}\int_0^a B_y(x)dx=\frac{\Phi_0}{da(k)}=\frac{\Phi_0}{dL_x}l, \tag{53}$$

with $l=(L_x/\lambda)/2kK(k)$. It is obvious that $\overline{B}=0$ for $J_{\rm ex}<J_c$. Then we can expect that the vortex-lattice formation is verified experimentally by observing the external current dependence of the mean magnetic field. In order to examine such a possibility, let us carry out an order estimate of the relevant quantities in our model system.

The interaction constant g_L is expressed by the radiative decay time τ_r of the exciton due to the indirect transition and the intensity of the weak laser light I_0,

$$g_L\simeq\left[\frac{\pi c^2\hbar^4}{2(\hbar\omega_L)^3\tau_r a_c^2}I_0\right]^{1/2}, \tag{54}$$

where a_c is the lattice constant. Assuming a set of parameter values as $\hbar\omega_L\approx E(\mathbf{K}=0)\sim 1.5\,\text{eV}$, $\tau_r\sim 10^{-6}\,\text{s}$, $a_c\sim 1\,\text{A}$, and $I_0\sim 1\,\text{W cm}^{-2}$, we have $g_L\sim 10^{-12}\,\text{erg cm}^{-1}$. Furthermore, as a typical case, we adopt a model system of the type-II quantum well in which the thickness is $L=15\,\text{A}$ and the exciton density $n_0\sim 10^{11}\,\text{cm}^{-2}$. From our result calculated in Sec. II, the exciton radius and the exciton-exciton interaction are given as $a_x\simeq 50\,\text{A}$ and $W\simeq 90\,\text{eV A}^2\simeq 1.4\times 10^{-26}\,\text{erg cm}^2$. In this model system, the conditions for our approximations to be applicable are satisfied as follows: $n_0 a_x^2\sim 10^{-2}\ll 1$ and $g_L/n_0^{3/2}W\sim 10^{-3}\ll 1$. Using these values of parameters, we have $\lambda\simeq 2\times 10^{-5}\,\text{cm}$ and the critical current $J_c\sim 3\,\text{mA cm}^{-1}$.

Now let us calculate the mean magnetic field. We consider the finite system with $L_x\sim 1\,\text{cm}$. The external current dependence of the mean magnetic field is shown in Fig. 8 by the solid line for our system with $L_x/\lambda\sim 10^5$. We also show the result for the case of $L_x/\lambda\sim 10$ by the dotted curve, to observe how the quantized behavior of the magnetic field appears in a hypothetical mesoscopic system.

As seen in Fig. 8, since L_x/λ is very large in our system, the number of vortices l seems to change its value continuously depending on $J_{\rm ex}$. With increasing $J_{\rm ex}$, the sharp rising of the magnetic field can be observed at $J_{\rm ex}=J_c$. The value of Φ_0/dL_x is estimated to be $\sim 10^{-7}\,\text{G}$ and $\overline{B}/(\Phi_0/dL_x)\sim 10^4$, as seen in Fig. 8; then the order of the mean magnetic field is to be $\overline{B}\sim 10^{-3}\,\text{G}$. From these results, it is concluded that the transition to the vortex-lattice phase can be verified experimentally by observing the external current dependence of the magnetic field.

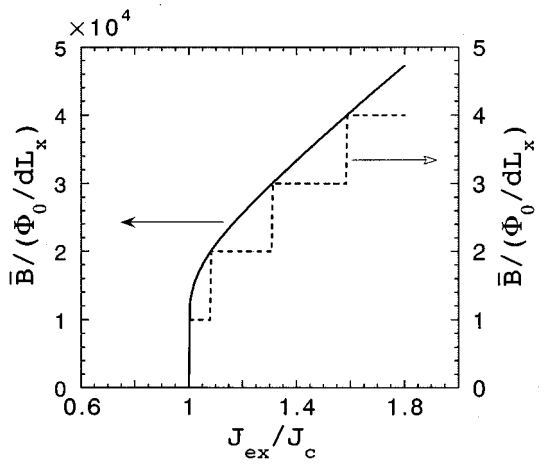

FIG. 8. The calculated magnetic field as a function of external current $J_{\rm ex}$. The sharp rising of the magnetic field at $J_{\rm ex}=J_c$ indicates the transition to the state where the superflow of excitons occurs in consequence of the vortex-lattice formation. The dotted line is for a hypothetical mesoscopic system (see text).

Finally it should be examined whether or not the velocity of the superflow v_s corresponding to $J_c\sim 3\,\text{mA}$ is smaller than the Landau critical velocity v_c. The velocity v_s is estimated to be $v_s\sim 2\times 10^5\,\text{cm/s}$, and the sound velocity u_s in the exciton system is to be estimated as $u_s=\sqrt{n_0W/M}\sim 2\times 10^6\,\text{cm/s}$. Then if we assume that the low-lying excitations consist solely of phonons, the condition $v_c\approx u_s>v_s$ will be satisfied. To obtain a decisive conclusion, further investigation of elementary excitations in our system is needed, which will be left to a future study.

[1] For recent reviews, see the relevant works in *Optical Nonlinearities and Instabilities in Semiconductors*, edited by H. Haug (Academic, New York, 1988); *Bose-Einstein Condensation*, edited by A. Griffin, D. Snoke, and S. Stringari (Cambridge University Press, Cambridge, 1995).

[2] H. Haug and S. W. Koch, *Quantum Theory of the Optical and Electronic Properties of Semiconductors* (World Scientific, Singapore, 1994).

[3] V. M. Galitzkii, S. P. Goreslavskii, and V. F. Elesin, Zh. Eksp. Teor. Fiz. **57**, 207 (1969) [Sov. Phys. JETP **30**, 117 (1970)].

[4] C. Comte and G. Mahler, Phys. Rev. B **34**, 7164 (1986).

[5] T. Iida, Y. Hasegawa, T. Higashimura, and M. Aihara, Phys. Rev. B **47**, 9328 (1993).

[6] See, for example, M. H. Anderson, J. R. Ensher, M. R. Matthews, C. E. Wieman, and E. A. Cornell, Science **269**, 198 (1665); K. B. Davis, M. O. Mewes, M. R. Andrews, N. J. van Druten, D. S. Durfee, D. M. Kurn, and W. Kitterle, Phys. Rev. Lett. **75**, 3969 (1995).

[7] D. W. Snoke and G. Baym, in *Bose-Einstein Condensation* (Ref. 1).

[8] D. W. Snoke and J. P. Wolfe, Phys. Rev. B **42**, 7876 (1990).

[9] E. Fortin, S. Fafard, and A. Mysyrowicz, Phys. Rev. Lett. **70**, 3951 (1993).

[10] A. Mysyrowicz, E. Fortin, E. Benson, S. Fafard, and H. Hanamura, Solid State Commun. **92**, 957 (1994).

[11] H. Hanamura, Solid State Commun. **92**, 957 (1994).

[12] I. Loustenko and D. Roubtsov, Phys. Rev. Lett. **78**, 3011 (1997).

[13] B. Link and G. Baym, Phys. Rev. Lett. **69**, 2959 (1992).

[14] A. E. Bulatov and S. G. Tikhodeev, Phys. Rev. B **46**, 11 058 (1992).

[15] G. A. Kopelevich, S. G. Tikhodeev, and N. A. Gippius, Zh. Eksp. Teor. Fiz. **109**, 2189 (1996) [Sov. Phys. JETP **82**, 1180 (1996)].

[16] M. Tsubota and T. Iida, in *Proceedings of the International Symposium on Quantum Fluids and Solids 'qfs'98* [Low Temp. Phys. **113**, 1165 (1998)].
[17] S. I. Shevchenko, Fiz. Nizk. Temp. **3**, 605 (1977) [Sov. J. Low Temp. Phys. **3**, 293 (1997)]; Phys. Rev. Lett. **72**, 3242 (1994).
[18] Z. S. Piao, M. Nakayama, and H. Nishimura, Phys. Rev. B **53**, 1485 (1996).
[19] H. Haug and S. Scmitt-Rink, Prog. Quantum Electron. **9**, 3 (1984).
[20] E. Hanamura and H. Hauge, Phys. Rep. **33C**, 209 (1977).
[21] A. I. Bobrysheva, V. T. Zyukov, and S. I. Beryl, Phys. Status Solidi B **101**, 69 (1980).
[22] O. Madelung, in *Semiconductor Basic Data*, edited by O. Madelung (Springer, Berlin, 1996).
[23] M. Tinkham, *Introduction to Superconductivity* (McGraw-Hill, New York, 1996).